Ab initio study of the $J^\pi = 0^\pm$ continuum structures in ^{4}He

S. Aoyama[1] and D. Baye[2]

[1]*Center for Academic Information Service, Niigata University, Niigata 950-2181, Japan*

[2]*Physique Nucléaire Théorique et Physique Mathématique, C.P. 229, Université Libre de Bruxelles (ULB), B 1050 Brussels, Belgium*

(Received 30 September 2017; published 3 May 2018)

The $J^\pi = 0^\pm$ continuum structures in ^{4}He are investigated by using an *ab initio* reaction theory with the microscopic R-matrix method. In the $E_x \gtrsim 20$ MeV excitation energy region of ^{4}He, the continuum states are mainly described by the $t+p$, $h+n$, and $d+d$ channels. The $J^\pi = 0^\pm$ elastic phase shifts of the $t+p$ and $h+n$ channels show an apparently resonant behavior which might indicate the existence of excited 0_3^+ and 0_2^- resonance states of ^{4}He above the known 0_2^+ and 0_1^- ones. However, the corresponding 0_3^+ and 0_2^- resonances have not been observed yet, although an experimental candidate with a large decay width is reported for 0_2^-. In this paper, by analyzing the $J^\pi = 0^\pm$ S matrices, we discuss why the observation of these states is unlikely.

DOI: 10.1103/PhysRevC.97.054305

I. INTRODUCTION

The ^{4}He nucleus has attracted much attention because it is an important building block in the nuclear system, which is often called the α cluster. It is strongly bound with respect to the four-nucleon threshold, $E = -28.296$ MeV, and the first excited state (0_2^+) lies at the high excitation energy $E_x = 20.21$ MeV [1]. This 0_2^+ level lies between the $t+p$ and $h+n$ thresholds and is considered as having a $3N+N$ (i.e., $\{t+p\}+\{h+n\}$) structure [2,3]. The triton (t) and ^{3}He (h) clusters are also known as important units in describing nuclear systems. Recently, *ab initio* reaction theories for more than three-body systems have been developed and applied to four-nucleons systems [4–9]. A benchmark calculation is performed for the $t+p$ and $h+n$ scatterings between the $3N+N$ and $d+d$ thresholds in Ref. [10]. Therefore, at present, one can quantitatively study the continuum structures of ^{4}He when investigating the $p+p+n+n$ system by using such an *ab initio* reaction theory. In a previous quantitative study, we have already shown that the long-standing problem of the flat behavior of the astrophysical S factor in $d(d,\gamma)^4$He is solved as an effect of the tensor part of the nucleon-nucleon interaction [4].

Experimentally, in the energy region below the $p+p+n+n$ threshold, nine excited states (0_2^+,0_1^-,0_2^-,1_1^-,1_2^-,1_3^-,2_1^-, 2_2^-,2_1^+) are reported in the compilation of the ^{4}He properties [1]. In our calculation with the realistic interactions AV8′+3NF and G3RS+3NF (see details in Ref. [5]), the phase shifts exhibit seven excited states (0_2^+,0_3^+,0_1^-,0_2^-,1_1^-,2_1^-,2_1^+). The calculated phase shifts for $1^\pm$ and $2^\pm$ were partly displayed in Ref. [5] and are not shown in the present paper. In a resonating-group calculation with the different realistic interaction AV18+UIX by Hofmann and Hale [11], similar phase shifts (corresponding to the seven resonance states) are also reported. There are no large ambiguities in the four-body system, when the two-nucleon realistic interaction reproduces very precisely the deuteron binding energy and the scatterings of two nucleons, and also, the three-nucleon interaction reproduces the binding energy of the three-nucleon systems.

Hofmann and Hale explain that the absence of observation of a 0_3^+ resonance originates from a coupling matrix element close to the unitary limit of the S matrix [11,12], i.e., from the smallness of the amplitude of the S matrix in the elastic channel. This mechanism of the small amplitude is also valid for 0_2^- as will be discussed in the present paper. But these authors suggest that the observed 0_2^- state may correspond to the calculated 0_2^- state, which would be rather inconsistent with the explanation for 0_3^+.

In order to obtain the S matrix, we calculate the matrix elements of the Hamiltonian by using the techniques of the correlated Gaussians plus the triple global representation (CG+TGV) [5]. The CG+TGV method is one of the most sophisticated versions of the so-called Gaussian expansion method (GEM) [13,14]. The GEM is also employed in a benchmark calculation of the ^{4}He ground state [15]. The original GEM cannot treat the asymptotic wave function because the Gaussian basis functions quickly damp in the asymptotic region. Therefore, together with the CG+TGV method, we employ the microscopic R-matrix method (MRM) to describe the asymptotic wave function [5,16,17]. The R-matrix approach [17] is also employed in another *ab initio* reaction theory, the no-core shell model with the resonating group method [18].

The purpose of the present paper is to investigate the unusual resonant-like behavior of the $J^\pi = 0^\pm$ phase shifts around $E_r^{t+p} \sim 6$ MeV, measured from the $t+p$ threshold. We do not investigate other spin states in this paper, because the phase shifts do not show any abnormal behavior [5]. We also discuss the complete (p,n) exchange reaction for these partial waves in a wide low-energy region ($E_x > 3$ MeV) of the ^{4}He spectrum.

The methods are described in Sec. II. The results of the calculations are given and discussed in Sec. III. A summary is presented in the last section.

II. METHODS

Here, we briefly summarize the CG+TGV and MRM methods. Details are given in Ref. [5]. The Hamiltonian of

 ©2018 American Physical Society

the four-body system is written as

$$\widehat{H} = \sum_{i=1}^{4} \widehat{T}_i - \widehat{T}_{\rm c.m.} + \sum_{i<j}^{4} \widehat{V}_{ij} + \sum_{i<j}^{4} \widehat{V}^C_{ij} + \sum_{i<j<k}^{4} \widehat{V}_{ijk}, \quad (1)$$

where $\boldsymbol{r}_i$ and $\widehat{T}_i$ are the coordinate and kinetic energy of the ith nucleon, $\widehat{V}_{ij}$ is the nuclear potential between nucleons i and j, and $\widehat{V}^C_{ij}$ is the Coulomb potential between them. The center-of-mass kinetic energy, $\widehat{T}_{\rm c.m.}$, is subtracted. We employ a typical realistic interaction called AV8′ [19], which is used by many authors. The AV8′ force has spin-orbit and tensor parts in addition to the central part. Furthermore, we introduce an empirical three-nucleon force (3NF) [2].

The wave function of ^{4}He is written as

$$\Psi_{JM} = \sum_{\alpha} c_\alpha \Phi^\alpha_{JM}(K) + \sum_{\beta} d_\beta \Phi^\beta_{JM}(H), \quad (2)$$

where K and H represent the type of Jacobi coordinates, and α and β are abbreviations of the channels in the K-type ($3N + N$) and H-type ($2N + 2N$) coordinates, respectively. For each α and β value, the partial wave functions take the form

$$\Phi^\alpha_{JM}(K) = \mathcal{A}\big[\big[\psi^{(1)}_{I_1}(\boldsymbol{x}_1,\boldsymbol{x}_2)\psi^{(2)}_{I_2}\big]_I \psi^{(3)}_l(\boldsymbol{x}_3)\big]_{JM} \times [[\tau^{(1)}\tau^{(2)}]_{T_{12}}\tau^{(3)}]_{T_{123}M_{123}}\tau^{(4)}_{\frac{1}{2}M_4}, \quad (3)$$

$$\Phi^\beta_{JM}(H) = \mathcal{A}\big[\big[\psi^{(1)}_{I_1}(\boldsymbol{y}_1)\psi^{(2)}_{I_2}(\boldsymbol{y}_2)\big]_I \psi^{(3)}_l(\boldsymbol{y}_3)\big]_{JM} \times [\tau^{(1)}\tau^{(2)}]_{T_{12}M_{12}}[\tau^{(3)}\tau^{(4)}]_{T_{34}M_{34}}. \quad (4)$$

The K-type coordinates are defined as $\boldsymbol{x}_1 = \boldsymbol{r}_2 - \boldsymbol{r}_1$, $\boldsymbol{x}_2 = \boldsymbol{r}_3 - (\boldsymbol{r}_1 + \boldsymbol{r}_2)/2$, $\boldsymbol{x}_3 = \boldsymbol{r}_4 - (\boldsymbol{r}_1 + \boldsymbol{r}_2 + \boldsymbol{r}_3)/3$, and the H-type coordinates are defined as $\boldsymbol{y}_1 = \boldsymbol{r}_2 - \boldsymbol{r}_1$, $\boldsymbol{y}_2 = \boldsymbol{r}_4 - \boldsymbol{r}_3$, $\boldsymbol{y}_3 = (\boldsymbol{r}_3 + \boldsymbol{r}_4)/2 - (\boldsymbol{r}_1 + \boldsymbol{r}_2)/2$. The channel spin I results from the coupling of the cluster spins I_1 and I_2, T_{12}, T_{34}, and T_{123} are isospins arising from various couplings, and l is a relative angular momentum. The basis functions $\psi^{(1)}_{I_1}$ and $\psi^{(2)}_{I_2}$ describe cluster wave functions (e.g., $[\psi^{(1)}_{I_1}(\boldsymbol{x}_1,\boldsymbol{x}_2)]_{I_1}$ represents a t configuration for the $t + p$ channel). The parameters for the basis functions in $\psi^{(1)}$ and $\psi^{(2)}$ are determined by the stochastic variational method (SVM) [14]. They are explained in Ref. [5]. The relative wave functions are assumed to be expressed by superpositions of Gaussian-type functions such as

$$\varphi^{(3)}_l(\boldsymbol{x}_3) = N_l x_3^l \exp\left(-\frac{x_3^2}{b_3^2}\right) Y_{lm}(\hat{\boldsymbol{x}}_3), \quad (5)$$

where N_l is a normalization factor. Parameter b_3 is given by the geometric progression $b_3 = b_3^{\rm min}\gamma^{i-1}$ ($i = 1,\ldots,N$). The minimum value $b_3^{\rm min}$ is 0.2 fm and the maximum value $b_3^{\rm max}$ is 20 fm.

The Gaussian asymptotic behavior in Eq. (5) is corrected by using the procedure of the MRM [4,5,16,17]. One obtains microscopically the R matrix elements $\mathcal{R}_{\alpha\alpha'}$, where α and α' represent open or closed channels. The details of the MRM are described in Refs. [5,16,17]. The S matrix is deduced from the R matrix as

$$S^{J\pi} = (\mathcal{Z}^*)^{-1}\mathcal{Z} \quad (6)$$

TABLE I. Channel spins and orbital momenta ($^{2I+1}l_J$) of the physical $t + p$, $h + n$, and $d + d$ channels for $J^\pi = 0^\pm$ with $l \leqslant 2$.

No.	channel \ J^π	0^+	0^-
1	$t(\frac{1}{2}^+) + p(\frac{1}{2}^+)$	$^1S_0$	$^3P_0$
2	$h(\frac{1}{2}^+) + n(\frac{1}{2}^+)$	$^1S_0$	$^3P_0$
3	$d(1^+) + d(1^+)$	$^1S_0$	$^3P_0$
4		$^5D_0$	

with

$$\mathcal{Z}_{\alpha\alpha'} \equiv I_\alpha(k_\alpha a)\delta_{\alpha\alpha'} - \mathcal{R}_{\alpha\alpha'}k_\alpha a I'_\alpha(k_\alpha a), \quad (7)$$

where $I(kr)$ is the incoming Coulomb wave, k is the wave number, and a is the channel radius. The matrix elements of the S matrix, where α is an entrance channel and α' is an exit channel, are expressed by their modulus and phase as

$$S^{J\pi}_{\alpha\alpha'} = \eta^{J\pi}_{\alpha\alpha'} e^{2i\delta^{J\pi}_{\alpha\alpha'}}, \quad (8)$$

where $\eta^{J\pi}_{\alpha\alpha'}$ and $\delta^{J\pi}_{\alpha\alpha'}$ are real. The elastic phase shifts $\delta^{J\pi}_\alpha \equiv \delta^{J\pi}_{\alpha\alpha}$ of channel α are defined by its diagonal elements $S^{J\pi}_{\alpha\alpha}$. The magnitude $\eta^{J\pi}_\alpha \equiv \eta^{J\pi}_{\alpha\alpha}$ of a diagonal element is not necessarily unity due to the coupling with other channels.

In Table I, we describe the channel spins ($^{2I+1}l_J$) of the physical $d + d$, $t + p$, and $h + n$ channels for $J^\pi = 0^\pm$ with $l \leqslant 2$. In the MRM, since the R matrix is obtained by connecting to two-body asymptotic wave functions, we do not directly treat the three-body asymptotic form as $d + p + n$ and the four-body one as $p + p + n + n$. In place of including $d + p + n$ and $p + p + n + n$, we employ the so-called pseudostates of deuteron breakup [5]. The pseudostates are discretized continuum states obtained after the diagonalization of the Hamiltonian matrix, which is a typical approximation including the effect of the continuum states and is also widely employed by several methods (e.g., CDCC [20]).

III. 0^+ AND 0^- CONTINUA

A. $J^\pi = 0^+$

For $J^\pi = 0^+$ of ^{4}He, the elastic phase shifts are plotted in Fig. 1. The solid, dashed, and dotted lines represent those of the $t + p$ ($^1S_0$), $h + n$ ($^1S_0$), and $d + d$ channels ($^1S_0$ for the lower line, $^5D_0$ for the upper line), respectively. The interaction is AV8′+ 3NF. The experimental 0^+_2 resonance is observed a little above the $t + p$ threshold at $E_r^{t+p} = 0.40$ MeV [1]. The corresponding 0^+ resonance state is clearly seen in the $t + p$ phase shift, which crosses $\pi/2$ at $E_r^{t+p} = 0.14$ MeV.

The $^1S_0$ phase shift of the $h + n$ channel exhibits an attractive behavior at ∼6 MeV, whereas that of the $t + p$ channel exhibits a repulsive behavior at ∼6 MeV. This resembles a typical resonant behavior of a phase shift in two open channels [21]. Therefore, one could naively expect that this would make a peak of the elastic cross section at ∼6 MeV. However, this is not true for this case as discussed later. Also, the corresponding 0^+ resonance has not been observed yet.

We now discuss the behavior of a resonant-scattering phase shift with a schematic two-open-channels model (only the

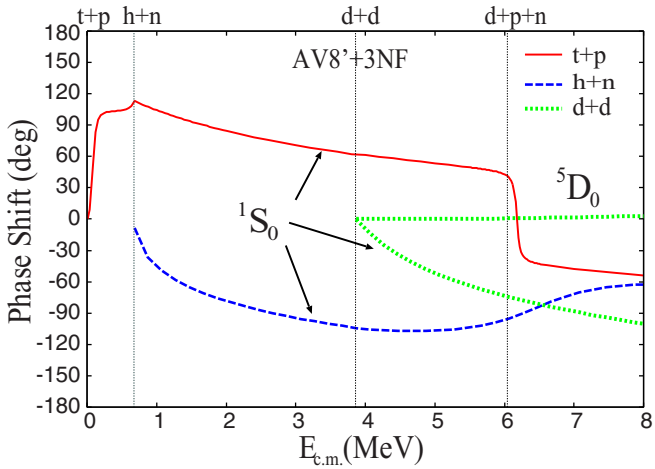

FIG. 1. 0^+ elastic phase shifts obtained with the AV8′+3NF interaction: $t+p$ (full line), $h+n$ (dashed line), and $d+d$ (dotted line) as a function of the $t+p$ center-of-mass energy.

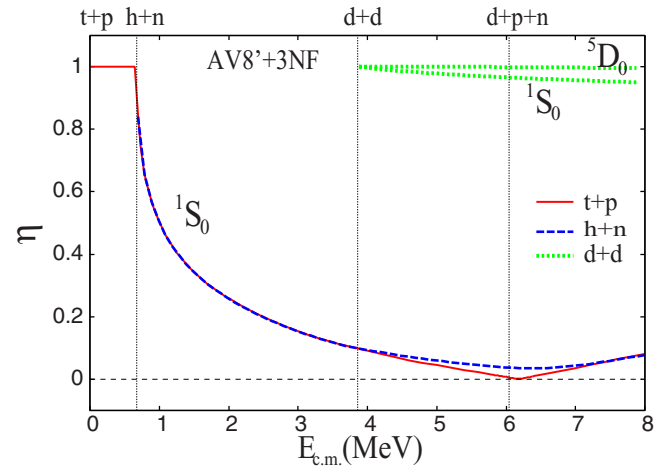

FIG. 2. Magnitudes η_α of the S matrix of 0^+ obtained with the AV8′+3NF interaction.

$t+p$ and $h+n$ channels). The S matrix at a resonance is written as [21]

$$S_{ii} = e^{2i\delta_i'(E)}\left(1 + \frac{i\Gamma_i}{E_r - E - \frac{1}{2}i\Gamma}\right), \tag{9}$$

$$= e^{2i\delta_i'(E)}\bar{S}_{ii}, \tag{10}$$

$$= \tau_i e^{2i(\delta_i'(E)+\bar{\delta}_i(E))}, \tag{11}$$

where the subscript i represents the channel, $i=1$ for the $t+p$ channel, and $i=2$ for the $h+n$ channel, δ_i' is a potential-scattering phase shift, $\bar{\delta}_i$ is a resonant scattering phase shift, Γ_i is a partial decay width, and $\Gamma = \Gamma_1 + \Gamma_2$ is the total decay width. The resonance part of the S matrix for $t+p$ is rewritten by introducing $x = \Gamma_1/\Gamma$,

$$\bar{S}_{11}(E) = \tau_1 e^{2i\bar{\delta}_1(E)}, \tag{12}$$

$$= (1-x) + x\frac{E - E_r - i\frac{\Gamma}{2}}{E - E_r + i\frac{\Gamma}{2}}. \tag{13}$$

The $\bar{S}_{11}$ matrix element behaves like a step function at $x=0.5$. The phase shift increases for $x > 0.5$ and decreases for $x < 0.5$ around the resonance energy E_r. It is noted that the magnitude of the S matrix τ_1 at the resonance energy is 0 for $x=0.5$ because of $\bar{S}_{11}(E_r) = 1-2x$. Thus, the observation of such a resonance is very difficult.

The calculated phase shifts ($\delta = \delta' + \bar{\delta}$) in Fig. 1 behave as those at $x \sim 0.5$. When the resonance lies at a high energy above the decay thresholds, it is not so strange that the partial decay width for $t+p$ has a similar value to that of $h+n$ because the essential difference between them is originating only from the Coulomb interaction.

In Fig. 2, we plot the magnitudes η_α of the S matrix for $J^\pi = 0^+$. The lines have the same meaning as those in Fig. 1. As seen from Fig. 2, the magnitude of the S matrix is $\sim$1 for the $d+d$ channels ($^1S_0$, $^5D_0$), which indicates a very weak coupling between the $3N+N$ and $2N+2N$ channels. The magnitude of the S matrix for the $t+p$ and $h+n$ channels becomes very small when the energy rises. Actually, $|\eta_{11}|^2$ is 5.1×10^{-5} at 6 MeV (Table II) for the $t+p$ channel, which means that the $t+p$ elastic scattering is completely forbidden in this partial wave.

It is also interesting that the magnitude of the S matrix is very small over a wide energy region, which means that the $t+p$ elastic scattering does almost not occur. In other words, one can expect that a complete (p,n) exchange reaction occurs above 3 MeV from the $t+p$ threshold in this partial wave, where $t+p$ is almost completely transformed into $h+n$. Although the results are obtained for the reverse reaction and with a different interaction, this is also expected from the benchmark calculation of Ref. [10] because the inelastic amplitude η of $h+n$ drops to zero with increasing energy (e.g., $\eta = 0.086$ at $E = 3.5$ MeV for AGS and FY, 0.074 for HH, see Table II and details in Ref. [10]).

In order to confirm the complete (p,n) exchange for 0^+, we display in Fig. 3 the Argand plot for the off-diagonal part of the S matrix S_{12}^{0+}. The left and right subscripts of the S matrix correspond to the entrance and exit channels, respectively. For 0^+, channel 1 is $^1S_0$ of $t+p$ and channel 2 is $^1S_0$ of $h+n$. As seen from Fig. 3, the modulus of S_{12}^{0+} becomes large when the energy is higher than 3 MeV and almost reaches the unit circle.

As described in Table II, the magnitude of the off-diagonal S matrix reaches the unitary limit, $|\eta_{12}|^2 + |\eta_{13}|^2 + |\eta_{14}|^2 \approx 1$. Due to the strong coupling, the diagonal part of the S matrix becomes zero. Thus, the 0^+ elastic scattering does almost not

TABLE II. Squared magnitudes of the S matrix.

Energy / η	4 MeV	5 MeV	6 MeV
$\lvert\eta_{11}\rvert^2$	0.0083	0.0020	5.124×10^{-5}
$\lvert\eta_{12}\rvert^2$	0.9881	0.9759	0.9666
$\lvert\eta_{13}\rvert^2$	0.0036	0.0220	0.0331
$\lvert\eta_{14}\rvert^2$	1.954×10^{-7}	5.561×10^{-5}	1.998×10^{-4}
$\sum_k \lvert\eta_{1k}\rvert^2$	1.0000	1.0000	1.0000

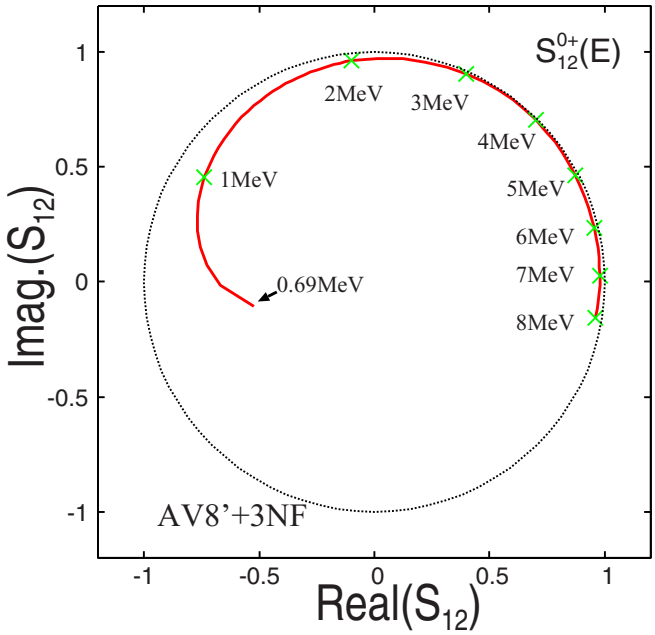

FIG. 3. Argand plot of S^{0+}_{12}. The initial channel is $t + p$ and the final channel is $h + n$.

occur in a wide energy region above 3 MeV. It is interesting to see that the maximum of η_{12} is realized around 4 MeV, which is different from the 6 MeV region for the minimum of η_{11} in Fig. 2. This can be understood by considering the coupling with the $d + d$ channel. Indeed, $|\eta_{13}|^2$ is as small as 0.0036 at 4 MeV, whereas $|\eta_{13}|^2 = 0.0331$ is larger at 6 MeV. Thus, $|\eta_{12}|^2 + |\eta_{13}|^2 + |\eta_{14}|^2$ at 6 MeV is larger than at 4 MeV, which makes $|\eta_{11}|^2$ at 6 MeV smaller.

To confirm the absence of effect from 0^+_3 on the cross section at ∼6 MeV, we investigate the so-called eigenphase shifts or eigenphases. The eigenphases are obtained when one diagonalizes the S matrix as

$$S^{J\pi}\mathbf{y}_k = e^{2i\delta_k^{J\pi}}\mathbf{y}_k, \tag{14}$$

where $\mathbf{y}_k$ is an eigenvector, eigenphase $\delta_k^{J\pi}$ is real, and $k = \{a,b,c,d\}$. Since the modulus of the eigenvalues of the unitary S matrix is unity, the anomaly of the phase shift discussed above does not appear.

In Fig. 4, we plot the eigenphases together with the elastic phase shifts (the same as in Fig. 1) in order to compare them. The suffix α for the elastic phase shift δ_α means $\{1,2,3,4\} = \{t + p, h + n, d + d, d + d\}$ as given in Table I. For the eigenphases, the relation with a physical channel is lost in principle because the physical channels are mixed through the diagonalization of the S matrix. Thus, the suffix $k = \{a,b,c,d\}$ in δ_k represents a mixing of the channels $\{t + p, h + n, d + d, d + d\}$. We observe that δ_a and δ_b are similar to δ_1 and δ_2, respectively. The phase shifts δ_c and δ_d are almost the same as δ_3 and δ_4, which is easily understood from $\eta \sim 1$ for the $d + d$ channels in Fig. 2. In Fig. 4, one cannot see any resonant behavior of the phase shifts except for the 0^+_2 resonance above the $t + p$ threshold.

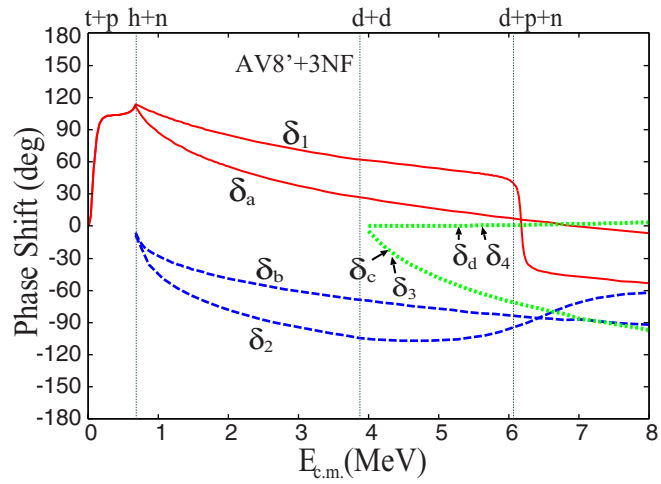

FIG. 4. 0^+ eigenphases. The elastic phase shifts in Fig. 1 are also plotted for comparison.

B. $J^\pi = 0^-$

In this subsection, we discuss the 0^- states of ^{4}He. Experimentally, two resonances, 0^-_1 ($T = 0$, $E_x = 21.01$ MeV, $\Gamma = 0.84$ MeV) and 0^-_2 ($T = 1$, $E_x = 25.28$ MeV, $\Gamma = 7.97$ MeV) are reported below the $p + p + n + n$ threshold [1]. The excitation energy is measured from the ground state of ^{4}He bound by 28.296 MeV. Since the observed 0^-_2 has a larger decay width ($\Gamma = 7.97$ MeV) than the resonance energies measured from the $3N + N$ thresholds ($E_r^{t+p} = 5.47$ MeV, $E_r^{h+n} = 4.71$ MeV), it would not make a peak in the cross section. Therefore, it is difficult to distinguish whether it is a true resonance of the four nucleons or the so-called responses of the continuum states due to the reaction mechanism [22,23].

Theoretically, two resonances, 0^-_1 and 0^-_2, have been predicted by the phase shift calculation of Ref. [11]. The calculated 0^-_1 state well corresponds to the observed 0^-_1 state. Hofmann and Hale suggest that the calculated 0^-_2 may correspond to the experimental 0^-_2 resonance with the large decay width [11]. This may be inconsistent with the discussion for the 0^+_3 state. If the 0^-_2 state is observed, there is not much reason why the 0^+_3 state is not observed, which was discussed in the previous section. In this subsection, we argue that the same mechanism of the zero magnitude of the S matrix also works for the 0^-_2 state.

For $J^\pi = 0^-$, the elastic phase shifts δ_α are plotted in Fig. 5 and the magnitudes η_α of the S-matrix elements in Fig. 6. The solid, dashed, and dotted lines represent the $^3P_0$ phase shifts of the $t + p$, $h + n$, and $d + d$ channels, respectively. A 0^-_1 resonance state is clearly seen at the $h + n$ threshold. The estimated energy is $E = -7.55$ MeV with respect to the four-body threshold [5], whereas the experimental energy is $E = -7.29$ MeV.

The $h + n$ and $t + n$ phase shifts also show a resonant-like behavior for two open channels at $E_r^{t+p} \sim 6.2$ MeV above the $t + p$ threshold. Therefore, one may think that it corresponds to the experimental 0^-_2 state at a glance. However, since the magnitude of the S matrix is almost zero at $E_r^{t+p} \sim 6.2$ MeV in Fig. 6 as in the case of 0^+_3 in Fig. 2, the elastic scatterings

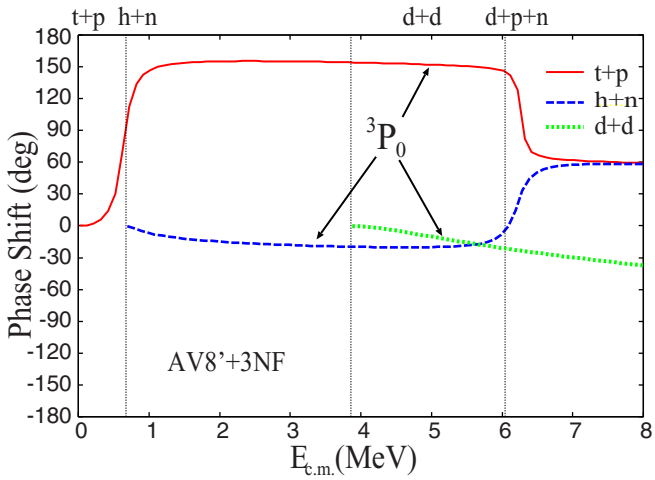

FIG. 5. 0^- elastic phase shifts obtained with the AV8'+3NF interaction: $t + p$ (full line), $h + n$ (dashed line), and $d + d$ (dotted line).

of $t + p$ and $h + n$ are almost forbidden in this partial wave. Thus, the observation of 0_2^- would be unlikely.

In Fig. 7, we display the Argand plot for the off-diagonal part of the S matrix, S_{12}^{0-}. Channel 1 is $^3P_0$ of $t + p$ and channel 2 is $^3P_0$ of $h + n$. As seen from Fig. 7, the modulus of the S matrix becomes large when the energy is high and almost reaches the unit circle above 4 MeV. Therefore, if the $t + p$ scattering of 0^- occurs above 4 MeV, it is almost completely transformed to $h + n$ as in the case of 0^+.

The eigenphases and the elastic phase shifts are displayed in Fig. 8. If the eigenphase shows a resonant behavior at $E_r = 6.2$ MeV, a 0_2^- resonance state may be observed as a peak of the cross section. The suffix α for the elastic phase shift δ_α means $\{1,2,3\} = \{t + p, h + n, d + d\}$ as given in Table I. In δ_a and δ_b, except for the 0_1^- resonance, a resonant-like behavior is not seen. Therefore, we conclude that an observation of such a 0_2^- resonance is as unlikely as in the discussion of 0_3^+.

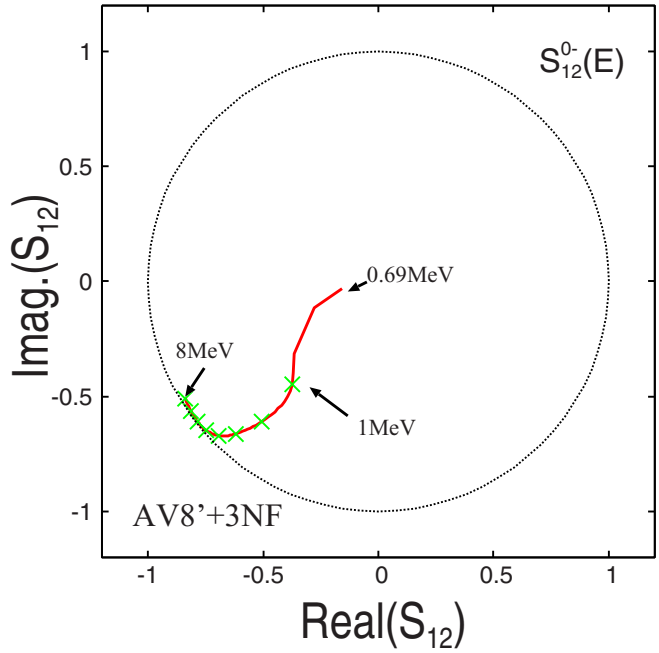

FIG. 7. Argand plot of S_{12}^{0-}. The initial channel 1 is $t + p$ and the final channel 2 is $h + n$.

IV. SUMMARY

By using an *ab initio* reaction theory with the MRM, we investigate the continuum structures of $J^\pi = 0^\pm$ in ^{4}He. Beyond the known 0_2^+ and 0_1^- resonances, the $J^\pi = 0^\pm$ elastic phase shifts for the $t + p$ and $h + n$ channels show a typical resonant behavior for two open channels. These states are candidates for the 0_3^+ and 0_2^- resonance states in ^{4}He, although the 0_3^+ state has not been observed yet. The difficulty of the observation is originating from the magnitude of the S matrix for the elastic channel which is almost zero.

Although the existence of the observed 0_2^- resonance state may be open to question because of its large decay width, it

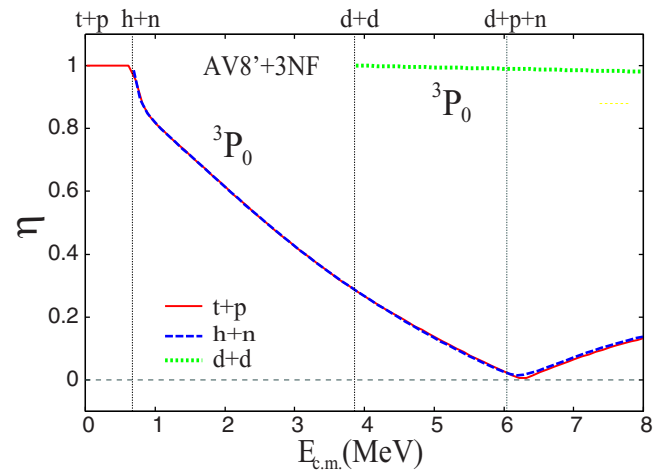

FIG. 6. Magnitudes η_α of the S matrix for 0^- obtained with the AV8'+3NF interaction.

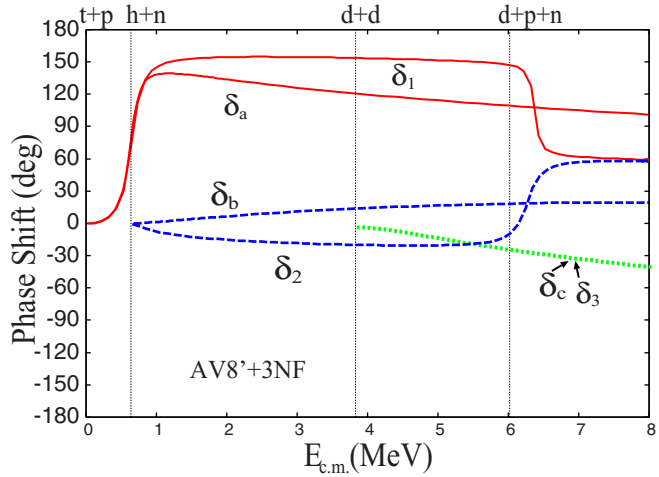

FIG. 8. 0^- eigenphases. The elastic phase shifts in Fig. 5 are also plotted for comparison.

is interesting to know whether the 0_3^+ resonance state is also observed as a large-decay-width state like 0_2^-. Both 0_3^+ and 0_2^- states of ^{4}He should be understood consistently. At least, the theoretical resonant structure is very similar for both states, as discussed in this paper.

Furthermore, we discuss the complete (p,n) exchange in the $J^\pi = 0^\pm$ partial waves, which is seen in a wide low-energy range of the $t + p$ reaction. A complete (n, p) exchange reaction would also occur in the $h + n$ reaction because of the unitarity of the S matrix. In the future, we will discuss how the cross section should be observed by using the present *ab initio* reaction theory with the MRM for higher partial waves.

ACKNOWLEDGMENTS

The authors would like to thank Prof. P. Descouvemont and Prof. Y. Suzuki for helpful discussions. This work used the Cray XC40 super computer at Yukawa Institute for Theoretical Physics in the Kyoto universityi and computational resources of the COMA supercomputing system provided by Interdisciplinary Computational Science Program in Center for Computational Sciences, University of Tsukuba.

[1] D. R. Tilley, H. R. Weller, and G. M. Hale, Nucl. Phys. A **541**, 1 (1992).
[2] E. Hiyama, B. F. Gibson, and M. Kamimura, Phys. Rev. C **70**, 031001(R) (2004).
[3] W. Horiuchi and Y. Suzuki, Phys. Rev. C **78**, 034305 (2008).
[4] K. Arai, S. Aoyama, Y. Suzuki, P. Descouvemont, and D. Baye, Phys. Rev. Lett. **107**, 132502 (2011).
[5] S. Aoyama, K. Arai, Y. Suzuki, P. Descouvemont, and D. Baye, Few-Body Syst. **52**, 97 (2012).
[6] J. Carbonell, A. Deltuva, A. C. Fonseca, and R. Lazauskas, Prog. Part. Nucl. Phys. **74**, 55 (2014).
[7] A. Deltuva and A. C. Fonseca, Phys. Rev. C **91**, 034001 (2015).
[8] M. Viviani, L. Girlanda, A. Kievsky, and L. E. Marcucci, Phys. Rev. Lett. **111**, 172302 (2013).
[9] R. Lazauskas, Phys. Rev. C **91**, 041001(R) (2015).
[10] M. Viviani, A. Deltuva, R. Lazauskas, A. C. Fonseca, A. Kievsky, and L. E. Marcucci, Phys. Rev. C **95**, 034003 (2017).
[11] H. M. Hofmann and G. M. Hale, Phys. Rev. C **77**, 044002 (2008).
[12] H. M. Hofmann, and G. M. Hale, Nucl. Phys. A **613**, 69 (1997).
[13] E. Hiyama, Y. Kino, and M. Kamimura, Prog. Part. Nucl. Phys. **51**, 223 (2003).
[14] Y. Suzuki and K. Varga, *Stochastic Variational Approach to Quantum-Mechanical Few-Body Problems*, Lecture Notes in Physics (Springer, Berlin, 1998), Vol. 54.
[15] H. Kamada, A. Nogga, W. Glöckle, E. Hiyama, M. Kamimura, K. Varga, Y. Suzuki, M. Viviani, A. Kievsky, S. Rosati, J. Carlson, S. C. Pieper, R. B. Wiringa, P. Navrátil, B. R. Barrett, N. Barnea, W. Leidemann, and G. Orlandini, Phys. Rev. C **64**, 044001 (2001).
[16] D. Baye, P.-H. Heenen, and M. Libert-Heinemann, Nucl. Phys. A **291**, 230 (1977).
[17] P. Descouvemont and D. Baye, Rep. Prog. Phys. **73**, 036301 (2010).
[18] S. Quaglioni and P. Navrátil, Phys. Rev. Lett. **101**, 092501 (2008).
[19] B. S. Pudliner, V. R. Pandharipande, J. Carlson, S. C. Pieper, and R. B. Wiringa, Phys. Rev. C **56**, 1720 (1997).
[20] M. Kamimura, M. Yahiro, Y. Iseri, Y. Sakuragi, H. Kameyama, and M. Kawai, Prog. Theor. Phys. Suppl. **89**, 1 (1986); M. Yahiro, T. Matsumoto, K. Minomo, T. Sumi and S. Watanabe, *ibid.* **196**, 87 (2012).
[21] K. Wildermuth and Y. C. Tang, *A Unified Theory of the Nucleus* (Vieweg, Braunschweig, 1977).
[22] B. V. Danilin, J. Thompson, J. S. Vaagen and M. V. Zhukov, Nucl. Phys. A **632**, 383 (1998).
[23] S. Aoyama, T. Myo, K. Katō, and K. Ikeda, Prog. Theor. Phys. **116**, 1 (2006).